Chapter 5

Structural variability of Ag(I) metal-organic networks: C–H···π and metal···π Interactions

Published in

J. Coord. Chem. 69:3(2016) 562–573

5.1. Introduction

Non-covalent interactions are vital for the existence of solid and liquid phases. [202,203] traditionally considered as weak forces, quantification of these interactions, which manage the molecular aggregation and determine the supramolecular assembly, is of fundamental interest. [204] Various type of non-covalent interactions has been attracted the attention of many researchers in recent years due to their prevalent presence and key role in several fields of science and technology, such as biology, nanotechnology and others.[205] Besides hydrogen bond, [205] there are other interactions present such as those involving aromatic rings, which include cation– π, [206] metal-cation−π, [207] anion– π, [208] π – π stacking, [209] and CH– π interactions. [210]

The cation−π interactions formed between a cation and an aromatic ring, are of outstanding importance in determining the structure and function of supramolecular assemblies from material science, catalysis to chemical biology. [206] The structural and energetic modulations of cation−π interactions have been shown as a function of several factors such as (a) size of the π system, (b) site of solvation, (c) nature of cation and π system, (d) presence of substituent, and (e) cooperativity with hydrogen bonding and π−π stacking. [209] However the metal cation···π interactions where a metal ion can be fixed in vicinity to an olefinic system of rigid chelating ligands, play an important role in nature, particularly in protein structure, molecular recognition, and enzyme catalysis. [211−218]

The CH– π interaction is the hydrogen bonds that take place between a soft acid (CH) and a soft base (π -system). [219-220] Chelate rings can be involved in CH– π interactions as hydrogen acceptors with organic moieties and in stacking interactions with aryl rings considering the planar chelate rings with delocalized p-bonds can have aromatic character. H. Masui, [221]

Bogdanovicet. al. [222] observed the CH– π interactions with chelate rings of coordinated porphyrin in transition metal porphyrinato complexes. This type of interaction accounts the stability of porphyrin containing proteins and may play some role in the function of these proteins. [223] Several theoretical studies have shown that the stabilization of the CH– π bond comes, essentially, from the dispersion energy. [224-227]

In continuation to our study on Ag (I) coordination polymers, [228-232] we tried to synthesize some networks having extensive non-covalent interactions, as such weak forces play decisive role in the formation of supramolecular networks with exceptional properties. [233-236] The organic ligands with -CO_2H, and -SO_3H groups are of special interest because they can adopt a variety of coordination modes and result in diverse multidimensional frameworks. [237-240] In this work, we used flexible aromatic dicarboxylate, 1,4-phenylenediacetic acid (H_2pda) as the starting building block, the networks of which have been largely investigated so far, [242-244] as (i) it can rotate freely around C(sp3)-C(sp2, on the carboxylate group) bonds forming various conformation which may provide various connection modes with metal ions; (ii) it can also provide potential sites of hydrogen bonding and π.....π stacking interactions to form complicated structures of higher dimensionalities; (iii) its de-protonation may be affected by different pH values, which will again have a crucial influence on network topology. [245]

Here in we report two new polymeric coordination compounds, [Ag_2(bpp)$_2$(Phdac)].5H_2O (**9**) and [Ag_2(bpp)(HSSal)] (**10**), using N-donor bpp and different flexible ligands such as H_3SSal and H_2Phdac . Both the synthesized complexes were characterized by IR-spectroscopy and X-ray single crystal structure analysis which shows coordination polymers of different dimensionality. Both the complexes display luminescence behavior at room temperature.

5.2 Experimental

5.2.1 Materials

Silver nitrate, 1,4-pheneylenediacetic acid, 5-Sulfosalicylic acid and 4,4'-trimethylene dipyridine were purchased from SIGMA-ALDRICH Inc. All the chemicals were used without further purification.

5.2.2 Physical Measurements

Spectroscopic data were collected as described in Chapter 3.

5.2.3 Synthesis

5.2.3.1 Synthesis of $[Ag_2(bpp)_2(Phdac)].5H_2O$ (9)

Silver nitrate (0.5 mmol, 0.0859 g), 1,4-pheneylene diacetic acid (0.5 mmol, 0.0485g) and 4,4'-trimethylene dipyridine (0.5 mmol, 0.099 g) were mixed into a 50 ml round bottom flask. 15 ml of deionized water were added to it and the whole mixture was stirred for 30 mints. After completion of the reaction a small amount of white compound was separated at the bottom of the flask. The compound was dissolved by drop wise addition of minimum amount of 25% aqueous NH_3 solution to get a transparent liquid. The clear solution was kept in dark for slow evaporation. Diffraction quality block colourless crystals were obtained after 7 days. The single crystals were collected by decanting the solution and were dried in air. Yield: 67 % Anal. Calc. (%) for $C_{36}H_{48}Ag_2N_4O_9$ (896.52): C, 48.23; H, 5.39; N, 6.25Found (%): C, 48.24; H, 5.38; N, 6.26. IR (cm^{-1}): 650(w), 999(w), 1079(m), 1168(w), 1212(w), 1292(w), 1381(s), 1417(w), 1559(m), 1649(m), 3457(broad).

5.2.3.2. Synthesis of [Ag_2(bpp)(HSSal)] (10)

A mixture of silver nitrate (84.5 mg, 0.5 mmol), 5-Sulfosalicylic acid (0.25 mmol, 0.0636 g) and 4,4'-trimethylene dipyridine (0.5 mmol, 0.099 g) in 10 ml deionised water was taken in a 50 mL round bottom flask. The reaction mixture was stirred for 30 mints at ambient temperature to get a turbid solution. Aqueous NH_3 solution (25%) was added drop-wise into the mixture with constant stirring to get a colourless transparent solution. The clear solution was kept in dark for slow evaporation. Diffraction quality block colourless crystals were obtained after 10 days. The single crystals were collected by decanting the solution and were dried in air. Yield: 62 % Anal. Calc. (%) for $C_{20}H_{18}Ag_2N_2O_6S$ (630.16): C, 38.12; H, 2.88; N, 4.45. Found (%): C, 38.10; H, 2.91; N, 4.46. IR (cm^{-1}): 602(m), 678(m), 734(w), 805(m), 897(w), 1009(w), 1034(s), 1080(s), 1126(m), 1182(w), 1212(w), 1268(w), 1385(m), 1426(m), 1488(m), 1604(w), 1635(w), 1940(w).

5.3X-ray Crystallography

Suitable single crystals of the title complexes were selected and tip-mounted on a hair in peruoroether oil on a Xcalibur, Sapphire3, Gemini ultra diffractometer. The crystals were kept at T = 120(2)K during data collection. Using Olex2 [193], the structures were solved with the olex2. solve [246] structure solution program, using the Charge Flipping solution method. The model was refined with the ShelXLMP-2012 [137] refinement package using Least Squares minimization. A summary of crystal data and relevant refinement parameters are given in Table 5.1. [CCDC 1402965-1402966]

Table5.1. Crystal data and structure refinement parameters for 9 and 10.

Structure	(**9**)	(**10**)
Empirical formula	$C_{36}H_{48}Ag_2N_4O_9$	$C_{20}H_{18}Ag_2N_2O_6S$
Formula Weight	896.52	630.16
Temperature (K)	120(2)	120(2)
Crystal system	Monoclinic	Monoclinic
space group	C2/m	$P2_1/c$
a, b, c (Å)	19.0007(5), 6.89469(18), 14.3292(3)	10.04598(14), 9.45787(12), 21.8700(3)
α, β, γ (°)	90, 96.716(2), 90	90, 103.0392(14), 90
Volume ($Å^3$)	1864.30(8)	2024.37(5)
Z / Density (calc.) (Mg/m^3)	2 / 1.597	4 / 2.068
Absorption coefficient (mm^{-1})	1.109	2.080
Crystal size (mm^3)	0.301 × 0.199 × 0.193	0.34 × 0.12 × 0.06
Θ max/º	28.97	27.995
Measured Refl.	8922	38613
Independent Refl.	2373	4901
Reflections Used	2199	4550
R_{int}	0.0358	0.0342
Parameters	161	281
GooF	1.089	1.070
Final R indices [I > 2σ(I)]	R1=0.0299, *w*R2=0.0662	R1=0.0212, *w*R2=0.0487

R indices (all data)	R1=0.0330, *w*R2=0.0678	R1=0.0242, *w*R2=0.0499
Largest diff. peak and hole ($e.Å^{-3}$)	0.846 and -0.410	0.455 and -0.352

5.4 Results and Discussion

5.4.1 Crystal structure of **9**

X-Ray diffraction analysis reveals that compound **9** is a 2-D layer coordination polymer constructed from 1,4-pheneylene diacetic acid and 4,4'-trimethylene dipyridine ligands. The acid ligand has crystallographically-imposed mirror symmetry. As shown in Fig.5.1, the Ag atom is coordinated by two carboxylate oxygen atoms from the 1,4-pheneylene diacetate anion [the distances: Ag(1)–O(4), 2.524(2)Å] and two nitrogen atoms from two 4,4'-trimethylene dipyridine ligands [the distances: Ag(1)–N(3), 2.288(2)Å; Ag(1)–N(21), 2.189(4)Å] in a distorted tetrahedral geometry. The 1D polymeric chain which propagates along (0 0 1) direction has been depicted in Fig.5.2.

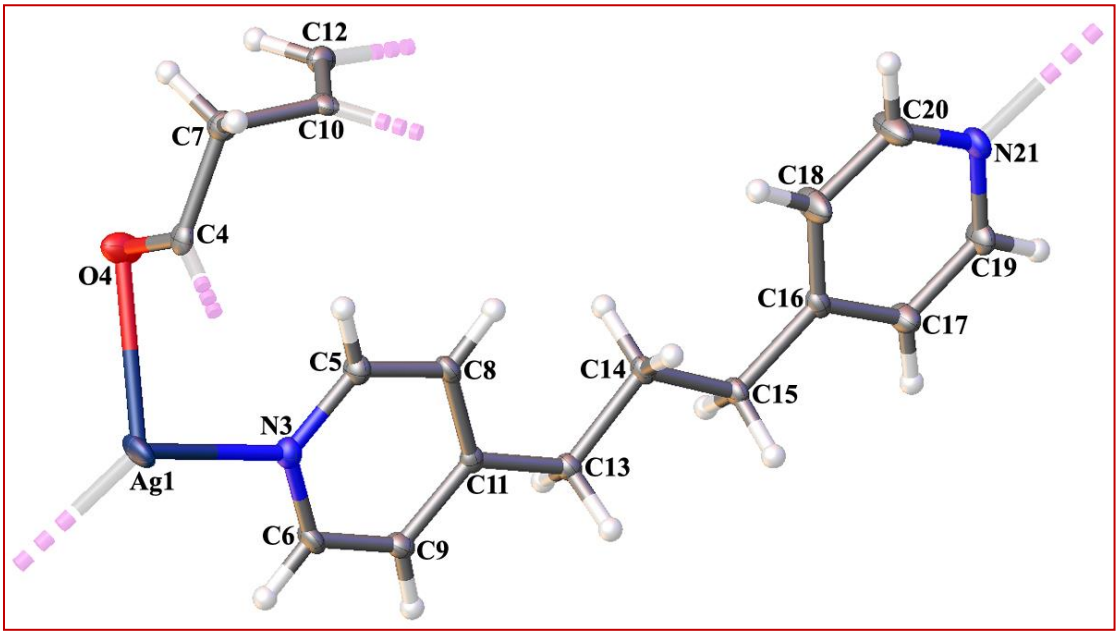

Fig. 5.1 Coordination environment and molecular view of **9** with atom numbering scheme. Solvent water molecules have been omitted for clarity.

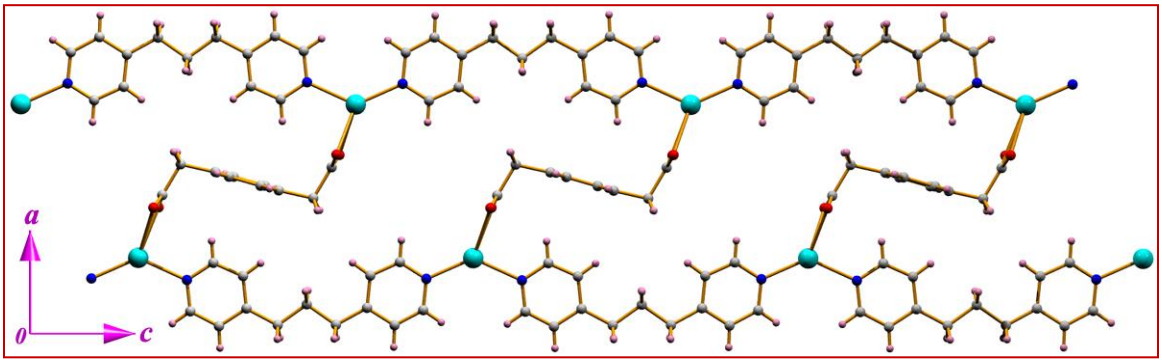

Fig. 5.2 Propagation of the 1D polymeric chain along (0 0 1) direction.

The parallel polymeric chains when viewed through *a*-axis, generates a layered architecture in **9**. The polymeric chains are stacked along (0 1 0) directions and the solvent water molecules have been utilized to direct the organization of Ag-polymeric units into hydrogen bonded layers (Fig.5.3a). The orientation of polymeric units is such that it simultaneously

facilitates self-complementary O–H···O interactions with adjacent layers which lead to optimal hydrogen-bonding with solvent water molecules (Table 5.2).

Table 5.2. Hydrogen bonding geometry of the title complexes (Å, °).

D–H···A	d(D–H)	d(H···A)	d(D···A)	D–H···A	Symmetry
Complex - 9					
O1–H1···O4	0.85	1.91	2.748(2)	169	1-x, y, 1-z
O3–H3A···O4	0.85	2.21	3.031(5)	161	1-x, y, 1-z
C9–H9···O1	0.93	2.41	3.238(4)	148	3/2-x, 1/2+y, 1-z
C15–H15A···O4	0.97	2.57	3.432(3)	148	3/2-x, 1/2+y, 1-z
C19–H19···O2	0.93	2.41	3.257(5)	151	3/2-x, 1/2+y, -z
Complex - 10					
O6–H6···O2	0.82	2.52	3.000(2)	118	x, 1+y, z
O6–H6···O5	0.82	1.91	2.618(2)	145	---
C2–H2···O6	0.93	2.56	3.337(2)	141	2-x, -1/2+y, 3/2-z
C3–H3···O2	0.93	2.30	3.155(3)	152	2-x, 1/2+y, 3/2-z
C8–H8···O1	0.93	2. 60	3.304(3)	133	---
C9–H9···O3	0.93	2.58	3.337(2)	139	1-x, 2-y, 1-z
C11–H11···O6	0.93	2.51	3.386(3)	158	x, 5/2-y, -1/2+z
C13–H13B···O3	0.97	2.48	3.327(3)	146	1-x, 2-y, 1-z
C20–H20···O3	0.93	2.47	3.207(3)	137	x, 3/2-y, -1/2+z

The solvent water molecule O1 at (x, y, z) acts as donor to the carboxylate oxygen atom O4 in the molecule at (1-x, y, 1-z), thus interconnects the parallel polymeric chains to build a 2D layer assembly in **9** (Fig. 5.3a). Due to the self-complementarity, another solvent water molecule O3 also interacting with the O4 atom for the strengthening of the assembly. Again, the C15 atom of the 4,4'-trimethylene dipyridine ligand in the molecule at (x, y, z) acts as donor to the carboxylate oxygen atom O4 in the molecule at (3/2-x, 1/2+y, 1-z), thus generating a 3D supramolecular framework in **9**; the parallel and central projection of the 3D architecture have been depicted in Figs. 5.3b and 5.4 respectively.

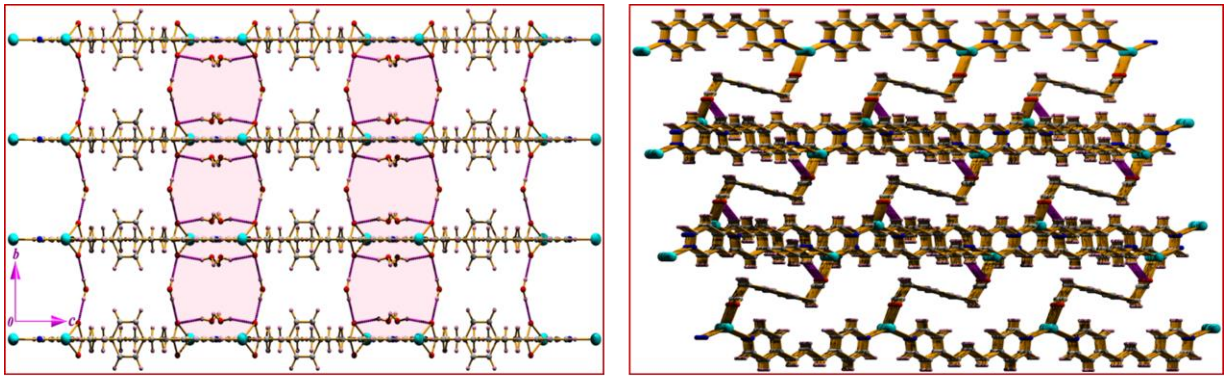

Fig. 5.3(a) Formation of the 2D layer architecture through O–H···O hydrogen bonding interactions in **9**. (b) Generation of the 3D architecture (Parallel view) in **9** through weak C–H···O hydrogen bonding interactions.

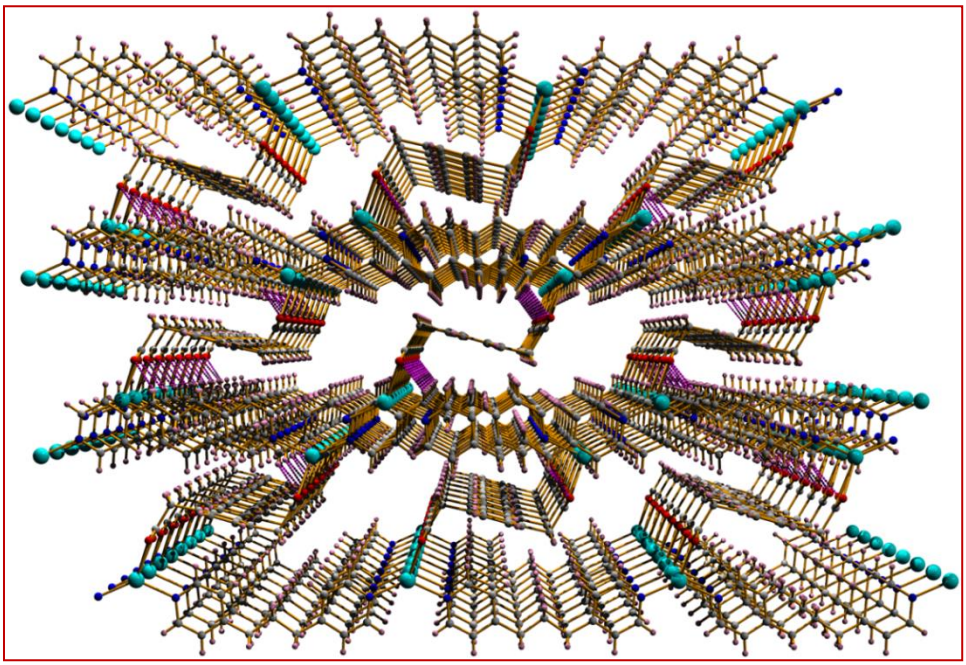

Fig. 5.4 The central projection of the 3D architecture in **9**.

In another structure, the carbon atom C14 is involved with the π-cloud of the pyridine ring (N3/C5/C8/C11/C9/C6) through weak C–H···π stacking interactions (Table 5.3) [247].

Table 5.3. Geometrical parameters (Å, °) for the C–H···π interactions.

D–H···A	d(D–H)	d(H···A)	d(D···A)	D–H···A	Symmetry
Complex - 9					
C14–H14A···Cg(2)	0.93	2.67	3.5047(6)	145	3/2-x, -1/2+y, 1-z
C14–H14A···Cg(2)	0.93	2.67	3.5047(6)	145	3/2-x, 1/2-y, 1-z
C14–H14A···Cg(2)	0.93	2.67	3.5047(6)	145	3/2-x, 1/2+y, 1-z
C14–H14A···Cg(2)	0.93	2.67	3.5047(6)	145	3/2-x, 3/2-y, 1-z
Complex - 10					
C12–H12···Cg(4)	0.93	2.56	3.436(2)	158	2-x, 2-y, 1-z

Cg(2) and Cg(4) are the centroids of the rings (N3/C5/C8/C11/C9/C6) and (C1/C2/C3/C4/C5/C6) respectively.

The C14 atom at (x, y, z) acting as donor to the centroids of the aryl ring at (3/2-x, -1/2+y, 1-z), (3/2-x, 1/2-y, 1-z) and (3/2-x, 3/2-y, 1-z) respectively, thus forming a 2D layered assembly in (1 1 0) plane (Fig. 5.5a). Most surprisingly, the metal atom Ag1 interacts with the π-cloud of the pyridine ring (N21/C16–C20) through a unique metal···π interactions in **9** (Table 5.4) which leads the molecules to build another layer network in the (0 1 1) plane (Fig. 5.5b).

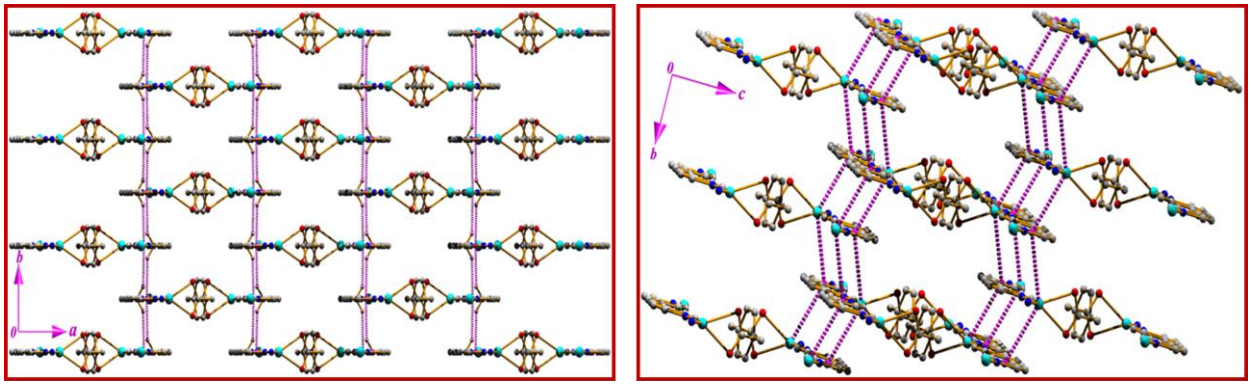

(a) **(b)**

Fig. 5.5(a) Formation of supramolecular layered assembly generated through C–H···π interactions in **9**. (b) Perspective view metal···π interaction in building layer network in (0 1 1) plane in **9**.

Table 5.4. Geometrical parameters (Å, °) for metal···π interactions.

Metal···Cg	Metal···Cg	Metal_Perp	β	Symmetry
Complex - 9				
Ag1···Cg(3)	3.78	3.447	24.20	3/2-x, -1/2+y, 1-z
Ag1···Cg(3)	3.78	3.447	24.20	3/2-x, 1/2+y, 1-z

Ag1···Cg(3)	3.78	3.447	24.20	3/2-x, 1/2-y, 1-z
Ag1···Cg(3)	3.78	3.447	24.20	3/2-x, 3/2-y, 1-z
Complex - 10				
Ag1···Cg(2)	3.868	3.613	20.92	2-x, 2-y, 1-z
Ag1···Cg(3)	3.911	3.497	26.59	1-x, 1/2+y, 1/2-z
Ag2···Cg(3)	3.845	3.016	38.34	1-x, 1/2+y, 1/2-z

For complex **9**, Cg (3) is the centroids of the ring (N21/C19/C17/C16/C18/C20) and for complex **10**, Cg(2) and Cg(3) are the centroids of the rings (N2/C8/C9/C10/C11/C12) and (N3/C16/C17/C18/ C19/C20) respectively.

Here, we have shown that the self-assembling tendency of suitable molecular building blocks through the unique metal···π interactions which have been utilized to drive the organization of coordination polymeric components into a supramolecular layer organization.

5.4.2. Crystal structure of 10

Complex **2** is also a 2-D coordination polymer constructed from 5-Sulfosalicylic acid and 4, 4'-trimethylene dipyridine ligands. The asymmetric unit contains two Ag(II) ions with different coordination environments, in which Ag(1) is triply coordinated while Ag(2) is four-coordinated with distorted tetrahedral geometry (Fig. 5.6).

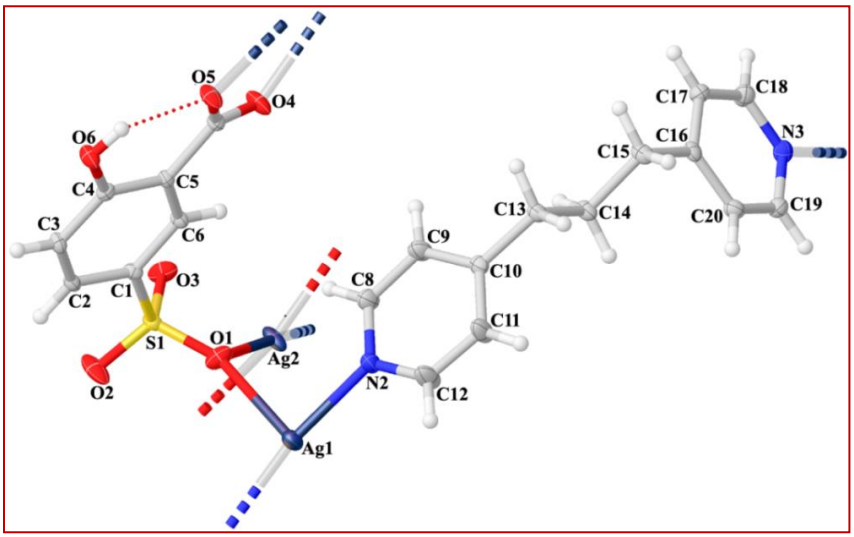

Fig. 5.6 Coordination environment and molecular view of **10** with atom numbering scheme.

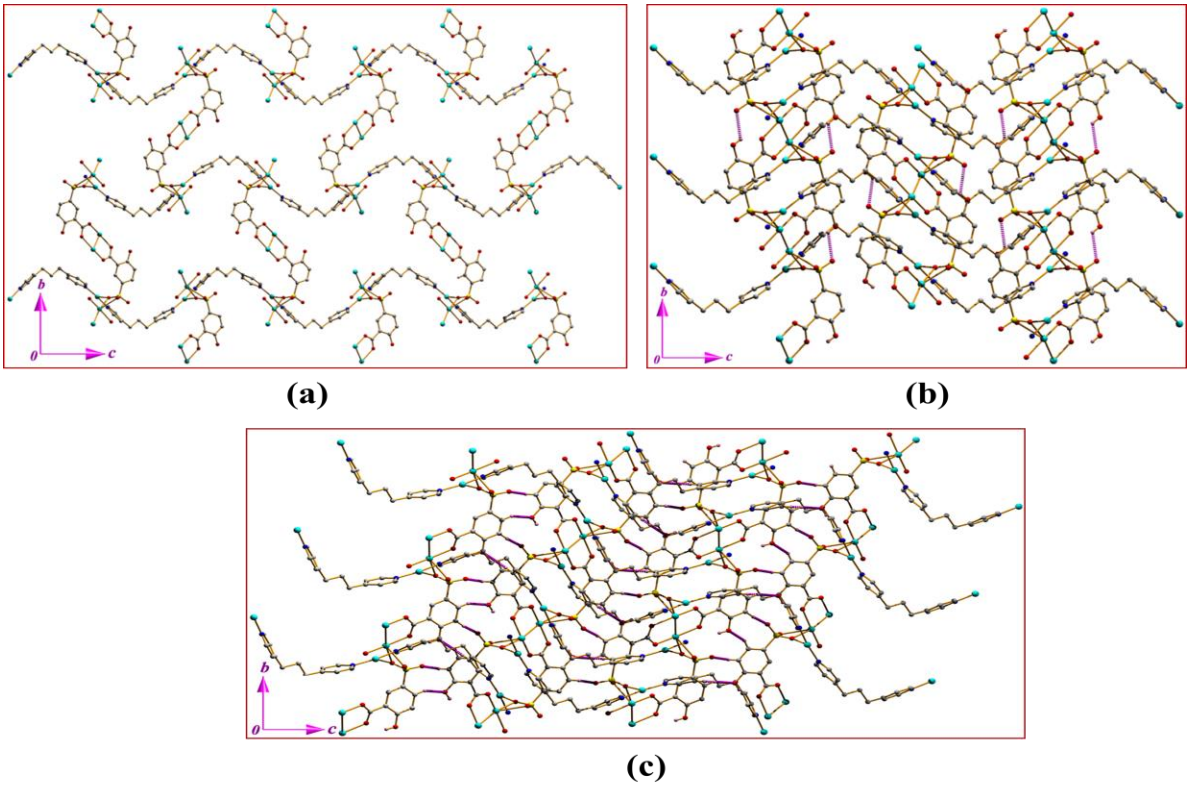

Fig. 5.7 (a) Formation of polymeric network in (0 1 1) plane in **10**. (b) Generation of 2D network in (0 1 1) plane through O–H···O hydrogen bonding interactions in **10**. (c) Generation of 2D network in (0 1 1) plane through C–H···O hydrogen bonding interactions in **10**.

Moreover, a two-dimensional network in **10** can also be visualized by considering the C−H···π (arene) bonds (Table 5.3) [248]. The pyridine ring carbon atom C12 in the molecule at (x, y, z) act as hydrogen bond donor to the aryl ring (C1–C6) in the molecule at (2-x, 2-y, 1-z), so generating a 2D layer network in (1 0 1) plane (Fig. 5.8a). Interestingly, both the metal ions Ag(1) and Ag(2) are in contact with the centroids of the pyridine rings through Ag···π interactions (Table 5.4). The Ag(1) atom is in contact with the pyridine rings (N2/C8–C12) and (N3/C16–C20) in the molecule at (2-x, 2-y, 1-z) and (1-x, 1/2+y, 1/2-z) respectively. Additional reinforcement between the Ag(2) ion with the centroid of the pyridine ring (N3/C16–C20) at (x, y, z) and (1-x, 1/2+y, 1/2-z), leads the molecules to build a unique layered network in the (0 1 1) plane (Fig. 5.8b).

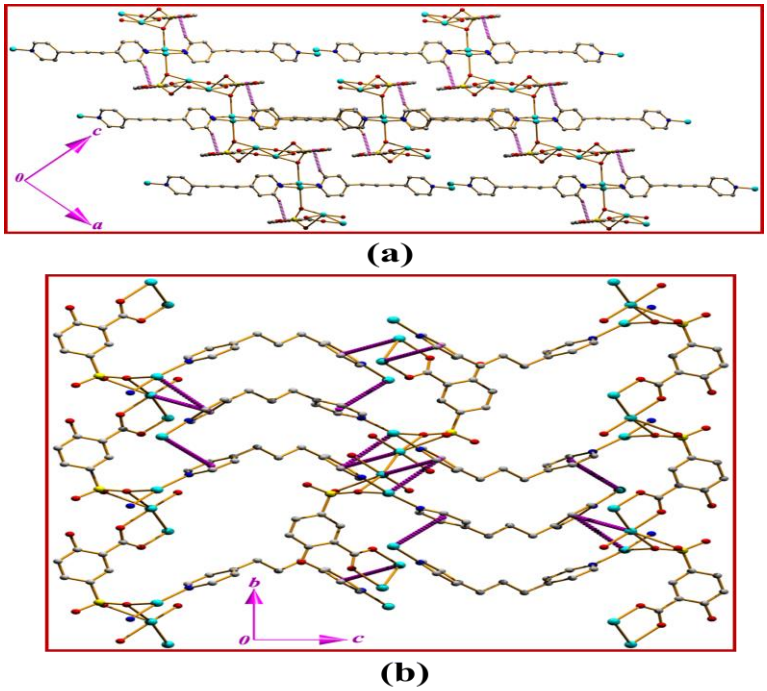

Fig. 5.8(a) Formation of supramolecular layered assembly in (1 0 1) plane through C–H···π interactions in **10**. (b) Formation of 2D layer network in (0 1 1) plane in **10**generated through metal···π interaction.

In this study, an in-depth analysis of the mode of operation of a number of noncovalent forces (hydrogen bonding, C−H···π and metal···π) simultaneously occurring in the crystal structures have been carried out, which fling some light on the cooperativity of the weak forces [249]. X-ray crystallography reveals that relatively stronger hydrogen bonding forces and comparatively weaker π-forces operate in a particular manner and the assemblies generated by them are extended in a layered orientation. The weak forces involved in the assembly, namely, C−H···π and metal···π interactions appear to be crucial and are probably responsible for rendering the present solid-state structure of the title complexes.

5.4.3 Luminescence study

The luminescent properties of **9**, **10** and the related free ligands 5-Sulfosalicylic acid (H_3SSA) and 4,4'-trimethylene dipyridine (bpp) was studied at room temperature. Complex **9** shows an emission maxima at 404 nm (λex=350 nm) (Fig. 5.10). The corresponding free bpp ligand displays emission band at 400 nm (λex=270 nm) (Fig. 5.9). However, H_3SSA shows emission maxima at 384 nm when excited with wavelength of 300 nm (Fig. 5.11). On the other hand, complex **10** shows a broad emission band with maximum at 394 nm (λex=280 nm) (Fig. 5.12). From these data it is evident that the emission band observed in complex **9** is slightly red shifted with respect to its corresponding bpp ligand in free State. Again, complex **10** is 10 nm red shifted with respect to the free 5-Sulfosalicylic acid (H_3SSA) and blue shifted by 16 nm with respect to the free 4,4'-trimethylene dipyridine (bpp) ligand . As Ag(I) ion is a d^{10} system so it is very difficult for this metal to get oxidized or reduced. Such emission behavior of **9** and **10** may be assigned to metal perturbed intra-ligand charge transfer transition. [228]

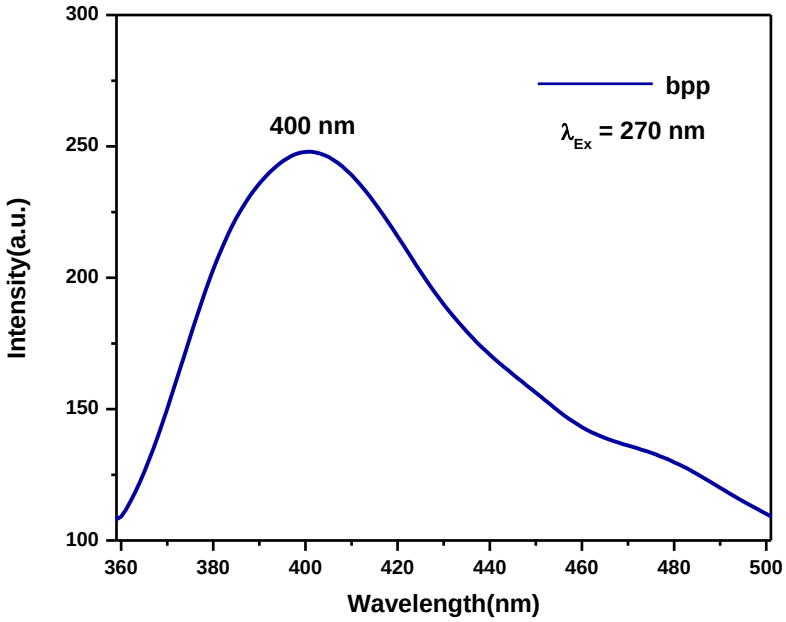

Fig. 5.9 Emission spectrum of 4,4'-trimethylene dipyramine, bpp (λ_{Ex} = 280 nm).

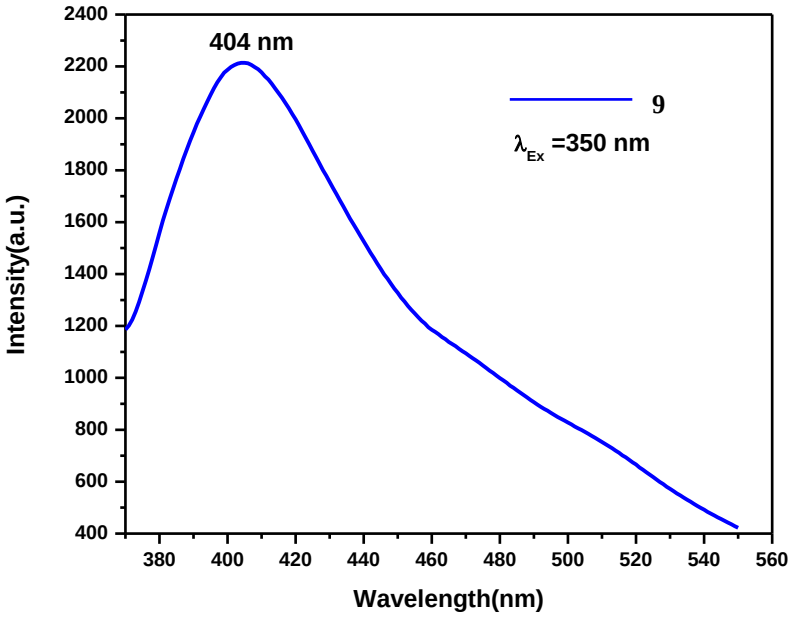

Fig. 5.10 Emission spectrum of **9** (λ_{Ex} = 350 nm).

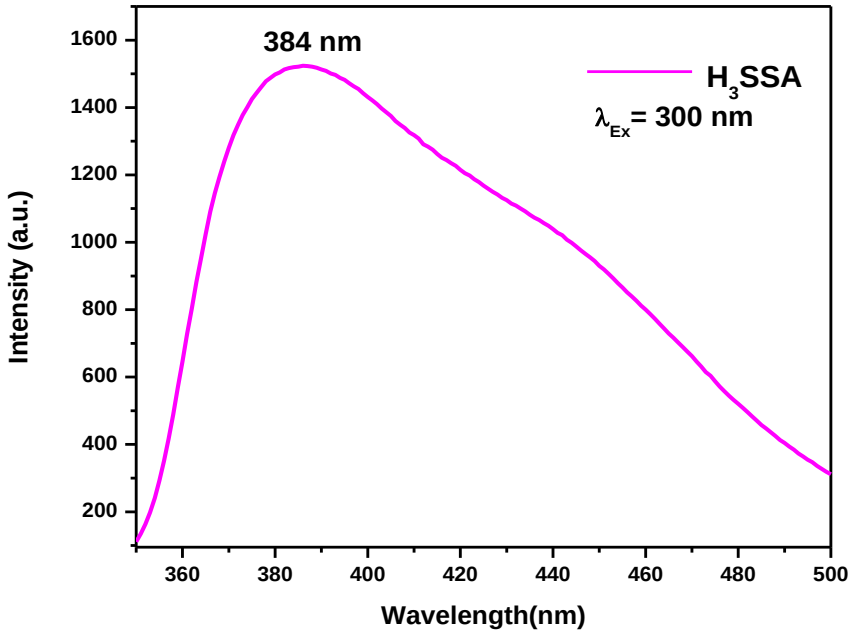

Fig. 5.11 Emission spectrum of 5-Sulfosalicylic acid, H_3SSA (λ_{Ex} = 280 nm).

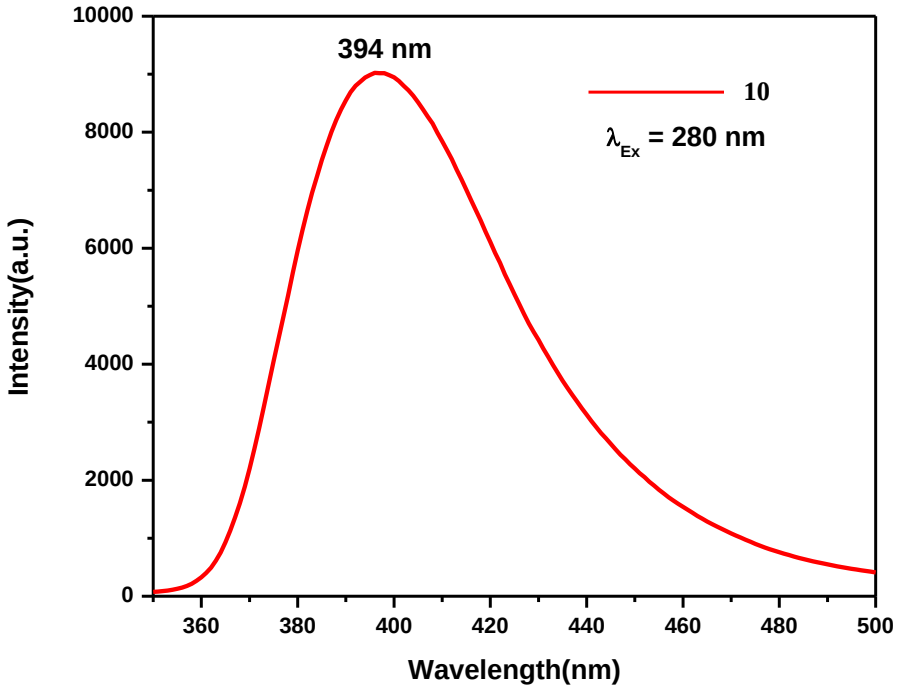

Fig. 5.12 Emission spectrum of **10** (λ_{Ex} = 280 nm).

5.4.4 IR study

The IR spectral analysis of complexes **9**-**10** shows a broad band in the region 3200-3500 cm^{-1}[ν(O-H)], suggesting the presence of H_2O molecules. ν_{as}(OCO), ν_s(OCO) bands (in cm^{-1}) appear at 1649, 1428 and 1635,1417 for **9** and **10**, respectively, indicating the involvement of carboxylate in the coordination.

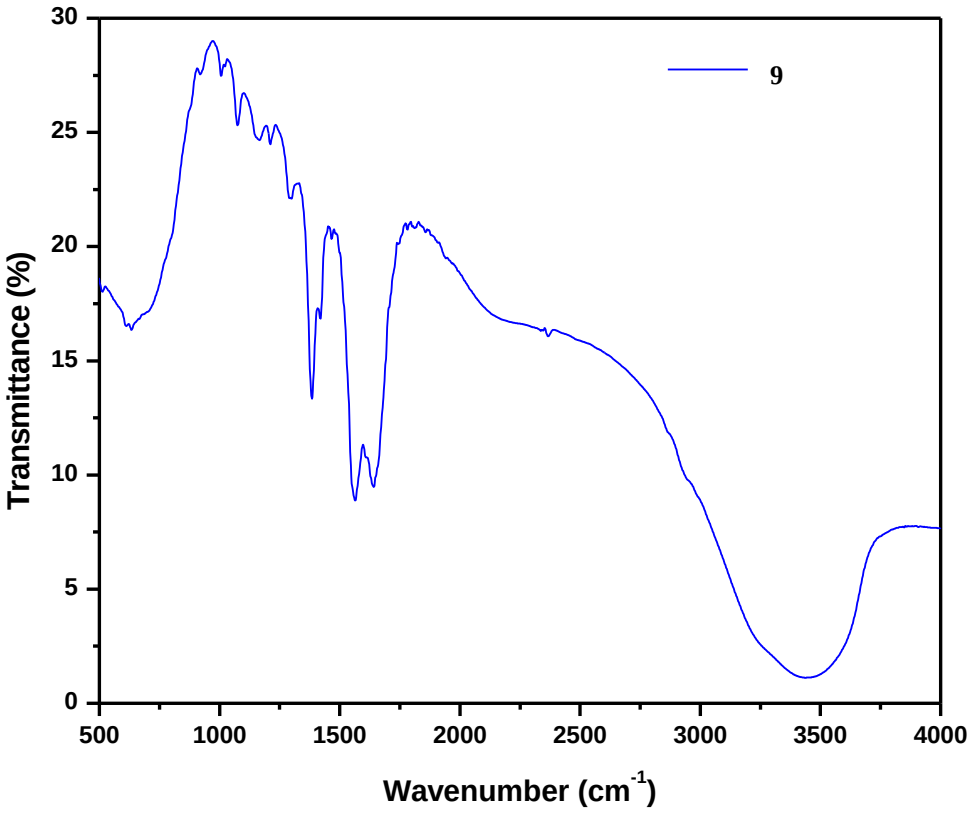

Fig. 5.13 IR spectrum of complex **9**

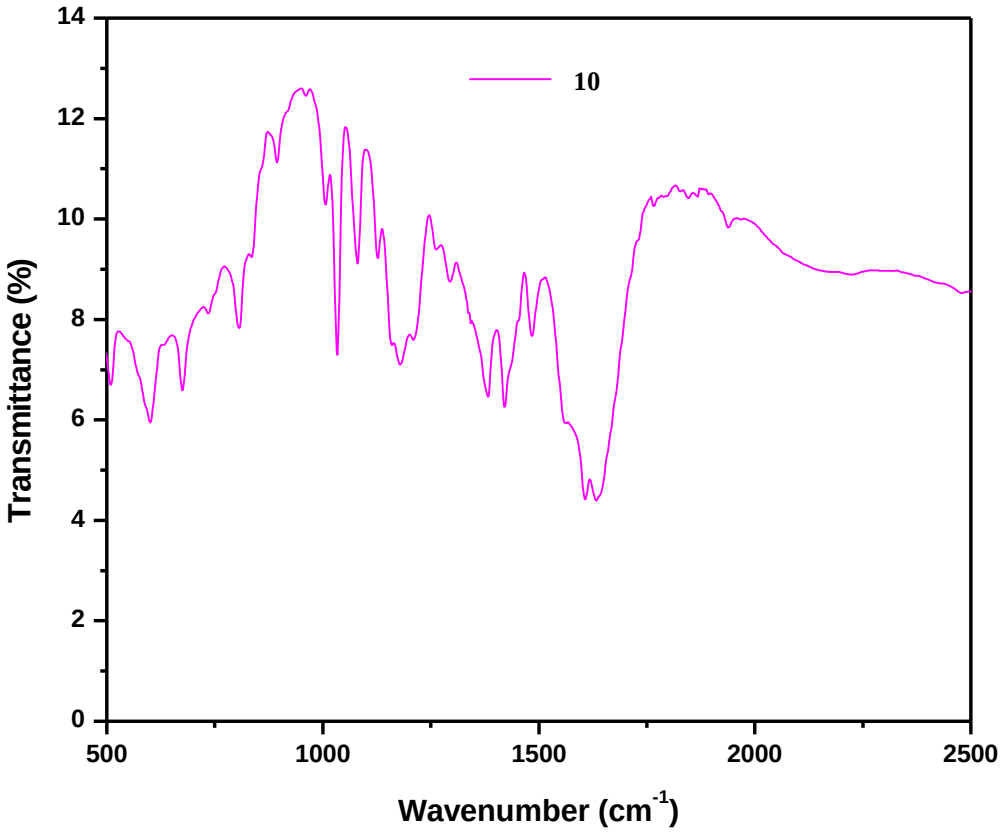

Fig. 5.14 IR spectrum of complex **10**